

ARTICLE

B. Lehmann · A. Dietrich · J. Heinhorst · N. Métrich
 M. Mosbah · C. Palacios · H.-J. Schneider
 A. Wallianos · J. Webster · L. Winkelmann

Boron in the Bolivian tin belt

Received: 6 August 1998 / Accepted: 19 August 1999

Abstract Tourmaline alteration and high boron contents are typical features of the magmatic-hydrothermal systems of the Bolivian tin province. The average boron content in melt inclusions of quartz phenocrysts from tin porphyry systems is 225 ppm (1 σ -variation range: 110–420 ppm; $n = 12$) and suggests a magmatic boron input to the hydrothermal tin systems, and not shallow post-magmatic leaching of boron from pelitic country rocks. Boron data from melt inclusions correlate positively with cesium, rubidium and arsenic, and negatively with lithium, titanium and zirconium, and define magmatic fractionation trends. The generally high B, As, Cs and Li contents in melt inclusions suggest involvement of pelitic source lithologies undepleted in these fluid-mobile

components, i.e. first-cycle metamorphic rocks. Magmatic fractionation modified the trace-element contents within a one-log-unit range. Bulk-rock Nd isotope data ($\epsilon_{\text{Nd}} -5$ to -10) are in agreement with the dominantly intracrustal geochemical signature of the Bolivian tin porphyry systems, but also imply a variable but minor mantle input. The metallogeny of the tin belt is likely a consequence of intracrustal melting of Lower Paleozoic pelitic and slightly carbonaceous source material, combined with an extended magmatic evolution. The long-lived thermal preparation of the root zones of the silicic systems is provided by mafic magma which also leaves a chemical imprint in the form of the hybrid dacitic bulk composition of the tin porphyry systems.

Editorial handling: F.M. Meyer

B. Lehmann (✉) · A. Dietrich · J. Heinhorst
 Institut für Mineralogie und Mineralische Rohstoffe,
 Technische Universität Clausthal,
 Adolph-Roemer-Strasse 2 A,
 D-38678 Clausthal-Zellerfeld, Germany
 e-mail: lehmann@immr.tu-clausthal.de

N. Métrich · M. Mosbah
 Laboratoire Pierre Sue, CEA-CNRS, CE-Saclay,
 F-91191 Gif-sur-Yvette, France

C. Palacios
 Departamento de Geología, Universidad de Chile,
 Casilla 13518, Santiago, Chile

H.-J. Schneider
 Ferdinand-Lehner-Strasse 4,
 D-84359 Simbach, Germany

A. Wallianos
 Max-Planck-Institut für Kernphysik,
 Saupfercheckweg 1,
 D-69029 Heidelberg, Germany

J. Webster
 Department of Earth and Planetary Sciences,
 American Museum of Natural History,
 New York, NY 10024-5192, USA

L. Winkelmann
 Bundesanstalt für Geowissenschaften und Rohstoffe,
 Stilleweg 2, D-30655 Hannover, Germany

Introduction

The metallogenic history of the central Andes during the last 200–250 Ma is characterized by punctuated regional episodes of ore formation on a general geotectonic background of quasi-continuous subduction along the South American convergent plate margin (Clark et al. 1976; Sillitoe 1976). Some of the most spectacular ore systems in this framework are the copper porphyry deposits of northern and central Chile, and the vein and porphyry deposits of the Andean tin belt of Bolivia and southernmost Peru. Both metal provinces represent short episodes of ore formation in narrow belts of more than 1000 km strike length. The most important Chilean copper porphyry systems developed in the time interval of 43–31 Ma (Collahuasi/Quebrada Blanca, Chuquicamata, La Escondida, El Salvador) and 10–4 Ma (Los Pelambres, Rio Blanco/Los Bronces, El Teniente) (Clark et al. 1998; Sillitoe 1988; Skewes and Stern 1995). The Andean tin belt hosts minor \sim 220 Ma old tin granite systems (Chacaltaya, Chojlla) and major 25–12 Ma old tin granite/porphyry systems (San Rafael, San José/Oruro, Llallagua, Cerro Rico de Potosí, Chorolque) (Grant et al. 1979; Fig. 1).

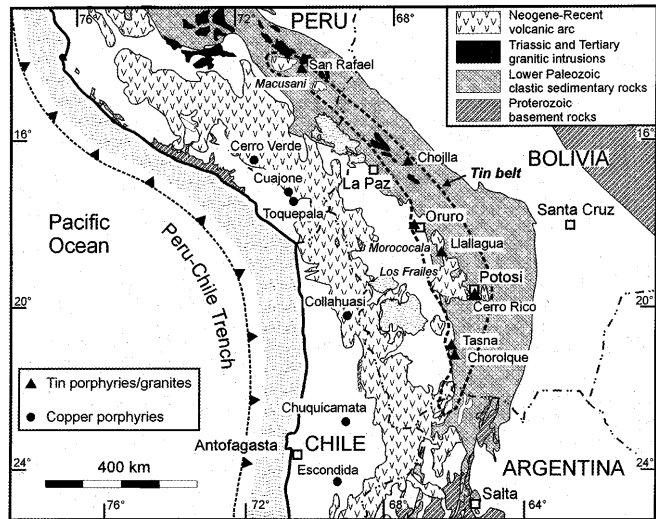


Fig. 1 Major ore deposits and geological framework of the central Andes

The Andean tin belt of Bolivia, SE Peru and northernmost Argentina (Fig. 1), usually known as the “Bolivian tin belt”, has a number of world class granite- and porphyry-related tin-bearing systems which are invariably characterized by a prominent hydrothermal tourmaline component. Tourmalinization defines the high-temperature centres of hydrothermal activity; tourmaline occurs as fine- to coarse-grained acicular crystals in veins and veinlets (open space filling), in greisens, hydrothermal breccias, including some pebble dykes, and as pervasive impregnation controlled by primary Al and Ca content (metasomatic replacement).

On a global scale, tin provinces have hydrothermal systems associated with granitic magmatism which are often either boron- or fluorine-rich (Taylor 1979). Examples of fluorine-rich tin provinces are the Erzgebirge, Nigeria, Mexico, and parts of the SE Asian tin belt, whereas the Cornwall and Bolivian tin provinces are boron-rich. The structural styles of mineralization in boron-rich environments are dominated by breccia pipes and stockworks, whereas the fluorine-rich environments have more passive apogranite/massive greisen systems (Pollard et al. 1987). The increased solubility of water in boron-rich melts compared to fluorine-rich melts (Manning and Pichavant 1988) may play a role in the structural evolution of these environments, with stronger release of mechanical energy in boron-rich melt systems. The development of spectacular decompression features with a wide spectrum of tourmaline breccias from the transitional magmatic-hydrothermal stage is particularly well known from Cornwall (Halls 1994). The boron specialization in tin provinces could be related to pelitic source lithologies because shales are about ten-times enriched in boron over average continental crust (Lehmann 1982).

We studied the boron distribution in non-altered Lower Paleozoic clastic rocks of the Eastern Cordillera of Bolivia, in tourmaline-quartz-sericite and chlorite

altered rocks of Bolivian tin ore systems, and in quartz-hosted melt inclusions of Bolivian tin porphyry systems. The melt inclusion work is limited to a relatively small data set and is of a reconnaissance nature. A more detailed account of the melt-inclusion geochemistry is presented by Dietrich (1999).

Analytical techniques

The whole-rock boron measurements were done by classical emission spectroscopy (pressed electrodes of rock powder and high-purity silver) and direct-coupled plasma spectroscopy (sodium hydroxide fusion). Reliability was checked by international rock standards and was within 5–15% error.

Boron microanalysis of melt inclusions was performed on hand-polished sections of quartz phenocrysts with a melt inclusion exposed at the surface of the quartz crystal. Boron analysis was carried out with the nuclear microprobe of Pierre Sue laboratory, Saclay, France, using the proton-induced nuclear reaction of $^{11}\text{B}(\text{p},\alpha)^{8}\text{Be}$ at a resonance energy of 660 KeV (Métrich et al. 1998). The samples were irradiated with an incident proton beam at 700 KeV, and the α -particles were detected with a 100 mm² surface barrier detector (100 μm depleted depth). The calibration in energy was made with a $^{233}\text{U}^{239}\text{Pu}^{241}\text{Am}^{244}\text{Cm}$ source, producing α -particles at 4.824, 5.157, 5.486, 5.805 MeV, respectively. The incident proton energy induces the following additional nuclear reactions: $^{7}\text{Li}(\text{p},\alpha)^{4}\text{He}$, $^{18}\text{O}(\text{p},\alpha)^{15}\text{N}$, $^{19}\text{F}(\text{p},\alpha)^{16}\text{O}$ which have to be taken into account for calibration. Further details are in Mosbah et al. (1995), Rio et al. (1995), and Métrich et al. (1998). The above Li reaction was used to estimate the lithium concentration, but the analytical setup is not optimal because of the resonance at 3 MeV. This results in a high analytical detection limit of 50–100 ppm Li and a large relative error. The limit of detection for boron is 10 ppm B. The boron and lithium data were cross-checked by secondary ion mass spectrometry (SIMS) using the Cameca IMS 3f ion microprobe at Woods Hole (Table 1). Analytical details are in Webster et al. (1997).

Additional trace elements were analyzed by proton-induced X-ray emission (PIXE) in Heidelberg with a proton microprobe with up to 2.5 MeV incident proton energy, and calibrated by a number of NIST standards and natural glasses (Traxel et al. 1995; Wallianos 1998). Major elements were analyzed by a Cameca SX100 electron microprobe (EMPA) in Clausthal (Dietrich 1999).

Regional background: boron in the Lower Paleozoic clastic sequence

The lithological framework of the Bolivian tin belt consists of a more than 10,000-m-thick intracratonic pile of clastic marine sedimentary rocks of Ordovician to Devonian age. The Lower Paleozoic sequence is structurally deformed, displays very low to low-grade metamorphism (Hercynian orogeny), and is locally unconformably overlain by outliers of Upper Mesozoic red beds and Lower Tertiary continental sedimentary and volcanic rocks.

A 50-km-long geochemical profile was taken perpendicular to the strike of the Cordillera Real by Lehmann et al. (1988). This section has 112 rock samples from about 5600 m of stratigraphic thickness from Middle Ordovician to Upper Silurian very low to low-grade meta-sandstones, meta-siltstones, and shales. The boron data define a bimodal distribution with a geo-

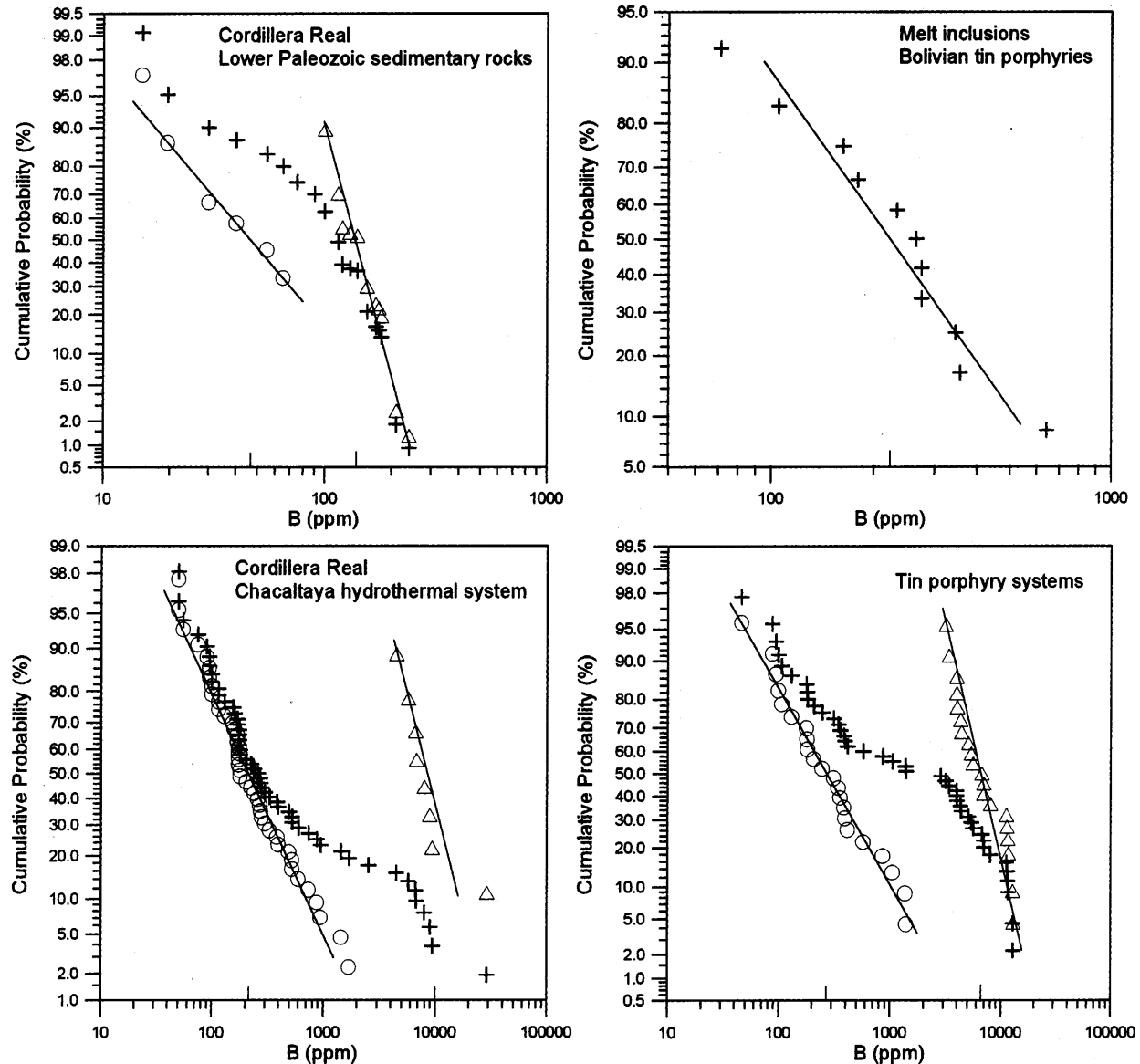


Fig. 2 Log-normal probability plots for boron data from Lower Paleozoic sedimentary rocks of the Cordillera Real, Bolivia (1), for the Triassic tin granite-related hydrothermal system from the Chacaltaya area, Cordillera Real, Bolivia (2), the Miocene tin porphyry systems of Llallagua, Chorolque and Cerro Rico de Potosí (3), and for quartz-hosted melt inclusions from the Llallagua, Chorolque and Cerro Rico de Potosí tin porphyries (4). The composite Lower Paleozoic boron population ($n = 112$) (crosses) can be divided into two subpopulations (circles) with a geometric mean of 130 and 45 ppm B, corresponding to pelitic (shale) and psammitic (siltstone/sandstone) samples, respectively. The sample population from the Chacaltaya tin system ($n = 52$) can be divided into two subpopulations with a mean of 10,000 and 210 ppm B, corresponding to the inner hydrothermal halo with very strong quartz-tourmaline alteration (quartz-muscovite-tourmaline-cassiterite greisen, and pelitic rock units partially transformed into tourmalinite), and the outer halo with chloritic alteration. The tin porphyry sample population ($n = 45$) breaks down into two subpopulations with 650 and 285 ppm B, corresponding to quartz-tourmaline alteration in core zones, and phyllitic alteration in higher and peripheral parts of porphyry intrusions/breccia pipes. The nuclear-reaction analysis/SIMS boron data from quartz-hosted melt inclusions ($n = 12$) define a geometric mean of 225 ppm B

metric mean of 45 ppm B in the sandstone/siltstone units (1σ -variation range: 20–95 ppm B) and a geometric mean of 130 ppm B in the shale units (1σ -variation range: 110–170 ppm B). These results correspond to global boron abundances for such rocks. It is interesting to note that the tin data from the same geochemical profile define a unimodal distribution with a mean of 4 ppm Sn (1σ -variation range: 3–7 ppm Sn), again similar to the crustal average. Some additional element abundances for the shale units are (versus quartzitic units in brackets): ca. 5 ppm Sb (ca. 0.5 ppm Sb), ca. 12 ppm As (ca. 5 ppm As) and ca. 15 ppm Cs (ca. 3 ppm Cs). Data are given as approximate geometric means because the data set is small (25 samples) and the variation range is large. The carbon content for Silurian metasediments was analyzed in a number of geochemical profiles in the Palca/Mururata area of the Cordillera Real by Winkelmann (1983). The mean C_{org} value is 0.3–0.7 wt% ($n = 200$).

Table 1 Selected trace-element data with 1σ -statistical error for melt inclusions from the Llallagua (L samples), Chorolque (C samples), and Cerro Rico de Potosí porphyries (P samples). Analyses by NRA (nuclear-reaction analysis), SIMS (secondary-ion mass spectrometry), and PIXE (proton-induced X-ray emission)

	B NRA	B SIMS	Li NRA	Li SIMS	Ti PIXE	As PIXE	Rb PIXE	Zr PIXE	Cs PIXE
C36-4	233 ± 29	220 ± 17	248 ± 71	198 ± 8	461 ± 3	47 ± 1	298 ± 2	85 ± 2	31 ± 11
P94b-2	162 ± 23	n.a.	71 ± 42	n.a.	583 ± 4	41 ± 14	486 ± 5	35 ± 3	<23
P95-3	265 ± 34	302 ± 18	189 ± 69	59 ± 3	415 ± 2	58 ± 1	398 ± 2	22 ± 1	194 ± 8
P97-3	643 ± 76	544 ± 27	35 ± 35	13 ± 5	271 ± 2	85 ± 1	637 ± 2	15 ± 1	167 ± 5
P97-6	346 ± 46	330 ± 21	n.a.	13 ± 5	348 ± 2	35 ± 1	416 ± 3	26 ± 1	76 ± 9
P97-4	179 ± 28	212 ± 17	n.a.	13 ± 5	576 ± 4	29 ± 1	423 ± 4	31 ± 3	68 ± 14
L24a-3	35 ± 5	47 ± 6	623 ± 80	559 ± 11	532 ± 4	12 ± 1	253 ± 3	36 ± 2	n.a.
L24a-2	105 ± 17	n.a.	520 ± 122	n.a.	585 ± 3	11 ± 1	254 ± 2	42 ± 1	<14
P95-4	n.a.	71 ± 8	n.a.	106 ± 4	428 ± 3	14 ± 1	292 ± 3	36 ± 3	20 ± 11
P97-2	n.a.	275 ± 19	n.a.	13 ± 5	n.a.	n.a.	n.a.	n.a.	n.a.
P95-1	357 ± 64	n.a.	264 ± 112	n.a.	329 ± 2	45 ± 1	488 ± 2	n.a.	101 ± 7
C44-2	275 ± 13	n.a.	n.a.	n.a.	176 ± 4	48 ± 2	301 ± 3	70 ± 4	29 ± 14

Boron in hydrothermal systems associated with tin granites and porphyries

The polymetallic hydrothermal systems of the Bolivian tin belt are associated with both the Permo-Triassic tin granites and the Middle Tertiary tin granites and porphyries (Clark et al. 1983; Evernden et al. 1977; Grant et al. 1979; McBride et al. 1983; Schneider and Lehmann 1977). Mineralization accompanies late-phase intrusive and hydrothermal activity characterized by satellite subintrusions, subvolcanic domes, hydrothermal breccias, and pervasive alteration with telescoped zoning patterns (Francis et al. 1983; Grant et al. 1980; Sillitoe et al. 1975). The two historically most important ore deposits of the tin belt are Cerro Rico de Potosí, which ranks as the largest historic silver producer in the world, and which, in its deeper sections, is also a major tin deposit, and Llallagua, which is probably the world's largest hard-rock tin deposit (Fig. 1). The principal current tin producer of the region, and the world's single largest tin mine (Amilot 1998), is the San Rafael mine in SE Peru which works a vein system in association with a 22–25 Ma multiple granite intrusion (Clark et al. 1983).

Both plutonic and volcanic rocks in the tin belt are mostly peraluminous, have high levels of lithophile trace elements such as Rb, Li, Cs, B and Sn, and belong to the ilmenite series (Pichavant et al. 1987; Erickson et al. 1990; Lehmann et al. 1990; Morgan et al. 1998). Boron enrichment is a characteristic and very widespread feature of the hydrothermal tin ore systems of both Triassic and Tertiary age. Early hydrothermal alteration consists chiefly of the mineral association quartz-sericite-tourmaline-pyrite. The hydrothermal mineral association of the ore deposits in the tin belt contains cassiterite as the dominant tin mineral and a variety of Ag, Sb, As, Cu, Pb, Zn and Bi sulfides, with locally elevated Au contents. Detailed accounts of the Bolivian ore systems are given by Ahlfeld and Schneider-Scherbina (1964), Grant et al. (1977, 1980), Kelly and Turneaure (1970) and Sillitoe et al. (1975, 1998).

Boron has been analyzed in a suite of 52 rock samples collected from the Chacaltaya hydrothermal system about 10 km north of La Paz. This hydrothermal system is centred on the 220-Ma Chacaltaya granite porphyry which is partly altered to quartz-muscovite greisen (Lehmann 1985). The boron data show a bimodal distribution pattern which can be divided into two subpopulations with means of 10,000 ppm B and 210 ppm B. The high-B sample suite is from the inner hydrothermal halo with strong quartz-tourmaline alteration (quartz-muscovite-tourmaline-siderite-cassiterite greisen and pelitic rock units partially transformed to tourmalinite), whereas the low-B suite is from the outer chloritic alteration halo.

Sixty-five rock samples from the Miocene tin porphyry systems of Llallagua, Chorolque, Cerro Rico de Potosí and San José/Oruro define a similar bimodal boron distribution with two subpopulations characterized by means of 6500 and 285 ppm B. These two sample sets are from quartz-tourmaline alteration in core zones and phyllitic alteration in higher and peripheral parts of porphyry intrusions/breccia pipes. Magma intrusion and high-temperature hydrothermal alteration are broadly synchronous and have been dated at 21 Ma for Llallagua (K-Ar; Grant et al. 1979), 14 Ma for Cerro Rico de Potosí (U-Th-Pb, Ar/Ar; Cunningham et al. 1996) and 16 Ma for Chorolque (K-Ar; Grant et al. 1979).

Boron in melt inclusions from tin porphyries

It is difficult to assess pre-eruptive compositions of melt systems by analyzing whole-rock samples because many magmatic constituents are volatile and because the primary characteristics of ore-bearing systems are invariably strongly disturbed by hydrothermal alteration. This is particularly true in the pervasively altered Bolivian tin porphyries. Consequently, we analyzed melt inclusions in quartz phenocrysts which are considered to represent a pre-eruptive stage of the magmatic systems. The phenocryst assemblage in the tin porphyries (quartz, largely

altered feldspars and biotite) constitutes about 50% of the rock, the remainder consisting of fine-grained groundmass with pervasive quartz-tourmaline-pyrite-sericite alteration in core zones of the systems, and a phyllitic and argillitic overprint of variable intensity over the full extents of the porphyry stocks.

The melt inclusions studied range in size from 10–50 µm, are subrounded to negative-crystal-shaped, and are randomly distributed within quartz phenocrysts. Melt inclusions in the Llallagua porphyry have shrinkage bubbles occupying about 5% of the inclusion volume. Larger shrinkage bubbles, up to 25 vol%, in the Chorolque and Cerro Rico porphyries indicate a simultaneous entrapment of vapor phase and/or loss of volatiles. In contrast to the glassy melt inclusions of the Chorolque and Cerro Rico systems, most melt inclusions in the Llallagua porphyry are strongly recrystallized and were rehomogenized in a tube oven at 800 °C for 24 h. Homogeneity was checked by microprobe element scans, elemental mapping and BSE images.

First results of electron and proton microprobe analyses of melt inclusions from the Bolivian tin porphyries are given by Dietrich et al. (1999). These data establish the melt inclusions as rhyolitic in composition with advanced degrees of fractionation, in striking contrast to the dacitic bulk-rock composition. The compositional gap between melt-inclusion and bulk-rock chemistry is interpreted to result from mixing of a rhyolitic magma, represented by the melt inclusions, and a mafic melt fraction which together produced the hybrid dacitic bulk composition (Dietrich et al. 1999).

Boron was analyzed in 12 melt inclusions from three tin porphyry systems, with most samples coming from Cerro Rico de Potosí (Table 1). The data from the Cerro Rico, Llallagua and Chorolque systems define a unimodal log-normal distribution with a geometric mean of 225 ppm B (1 σ -variation range: 110–420 ppm). The maximum value in the Cerro Rico melt inclusions is 640 ppm B.

The high boron contents are consistent with the generally highly-fractionated composition of the melt inclusions, as shown by multielement variation plots (Fig. 3). Boron correlates positively with arsenic, cesium and rubidium, but correlates negatively with lithium, zirconium and titanium.

The boron contents in the melt inclusions from the Bolivian tin porphyries are slightly higher than those from the central Bolivian Morococala volcanic field (Morgan et al. 1998) and the Mexican tin rhyolites (Webster et al. 1996), but similar to the extremely fractionated melt inclusions in pegmatitic quartz from the Ehrenfriedersdorf tin deposit, Germany (Webster et al. 1997). The highly evolved character of the melt inclusions in the tin porphyries may be compared with that of the highly fractionated tuffs and obsidian glasses of the Macusani volcanic field, SE Peru (Fig. 3).

The trends shown in Fig. 3 are interpreted as an expression of intramagmatic evolution by crystal-liquid fractionation, but the generally high abundances of

boron, lithium and arsenic are indicative of distinct source lithologies or processes (see below).

Discussion

The strong boron signature in the Bolivian tin porphyries may be the result of one or more of the following processes:

- Influx of slab-derived mantle fluids
- Partial melting of pelitic source material
- Magmatic differentiation processes
- Hydrothermal leaching of boron from pelitic country rocks

Boron enrichment in arc lavas is often considered the result of fluid infiltration from subducting slabs (Leeman and Sisson 1996). This assumption is based on the observation of anomalous boron contents in altered oceanic crust, high boron concentrations in pelagic sediments and the assumption of high boron solubility in moderate- to high-temperature aqueous fluids (Leeman and Sisson 1996). Smith et al. (1995) estimated averages of about 5 ppm B for the total oceanic crust, about 26 ppm B for the uppermost basaltic layer and about 53 ppm B for oceanic sediments. Young arc lavas often have correlated B and ^{10}Be enrichments which suggest a subduction origin for both components (Morris et al. 1990). Cross-arc transects show that boron contents normalized to immobile element abundances are highest in lavas from the volcanic front and decrease towards back-arc regions (Morris et al. 1990; Ryan et al. 1995, 1996). It is inferred that the cross-arc decrease in boron abundance reflects selective mobilization and progressive removal of boron from the uppermost slab portion via aqueous fluids released during prograde dehydration reactions. The elements Sb, As and Cs show typically trends similar to that of boron (Ryan et al. 1995).

However, these considerations apply to calc-alkaline andesitic rocks with boron concentrations generally in the range of less than 10 up to a maximum of 50 ppm. The high boron abundances in the Bolivian back-arc melt systems are difficult to explain strictly by slab-related processes, because the boron component in the subducting slab can be expected to be extracted at shallower depths near the magmatic front. This kind of boron enrichment can probably be seen in the Chilean and Peruvian coastal copper and gold systems which locally have tourmaline alteration, but generally to a much lesser degree than the Bolivian tin systems. Examples include the Miocene copper porphyry systems of Los Pelambres, El Teniente, Rio Blanco/Los Bronces and Toquepala (Skewes and Stern 1995; Atkinson et al. 1996; Serrano et al. 1996), the Early Tertiary breccia pipe copper deposits of northern and central Chile (Sillitoe and Sawkins 1971) and the mesothermal gold systems related to oxidized granites of Upper Jurassic to Lower Cretaceous age in the Coastal Cordillera of central Chile (Palacios et al. 1999).

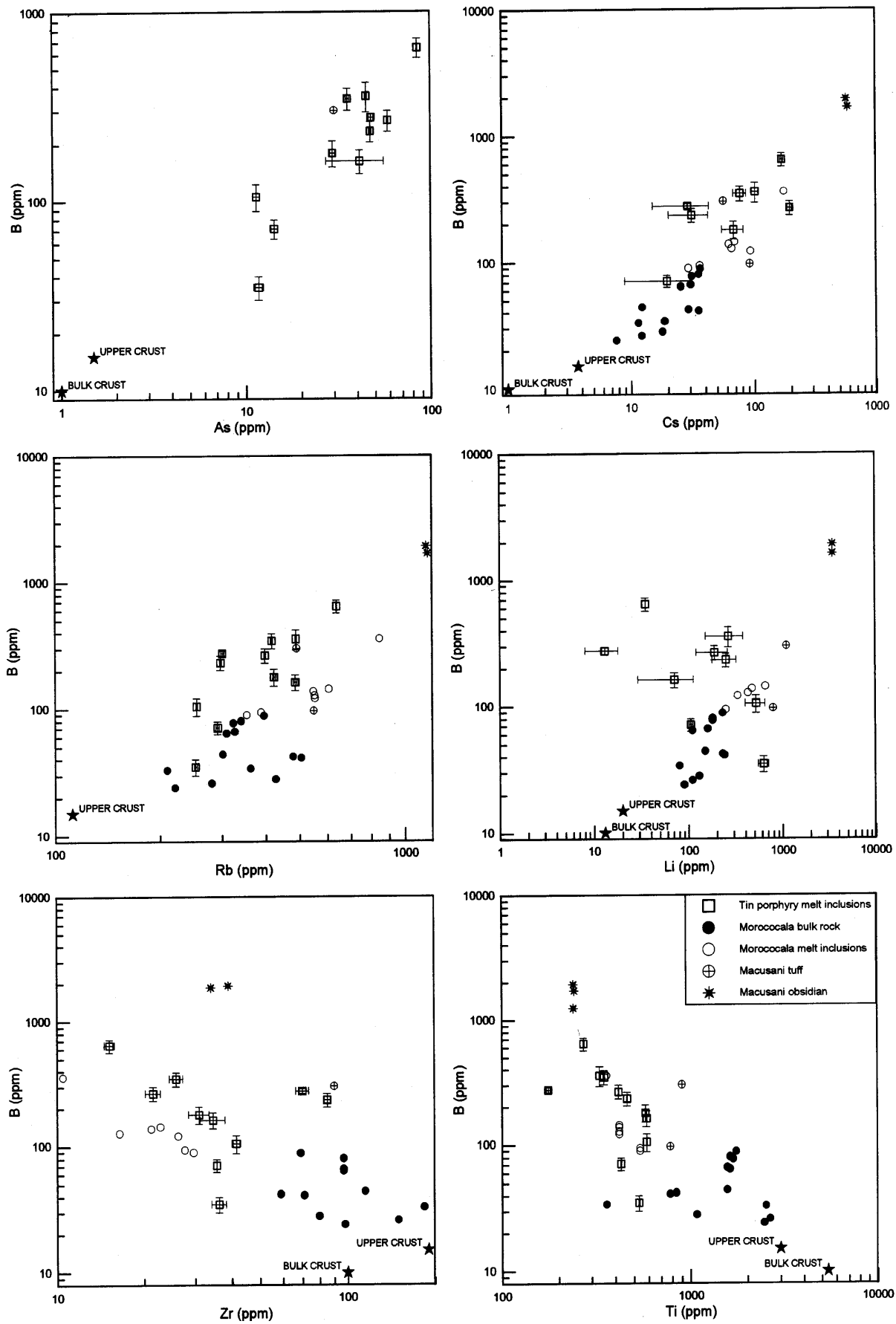


Fig. 3 Multielement variation plots for boron, lithium, arsenic, cesium, rubidium, zirconium and titanium abundances in quartz-hosted melt inclusions from the Llallagua, Chorolque and Cerro Rico de Potosí tin porphyry systems. Reference data are from the Macusani obsidian and ash-flow tuffs, SE Peru (Noble et al. 1984; Pichavant et al. 1987), and from the Morococala volcanic field in central Bolivia (Morgan et al. 1998). Continental upper-crust and bulk-crust compositions from Taylor and McLennan (1985)

The element suite in Fig. 3 displays systematic variation trends which align with non-altered bulk-rock and obsidian data from the 10–4 Ma old Macusani ignimbrite (Noble et al. 1984; Pichavant et al. 1987) and with bulk-rock and melt inclusion data from the rhyolitic to quartz-latic volcanic sequence of the 8–6 Ma Morococala field in central Bolivia (Morgan et al. 1998). The positive correlation of boron with incompatible elements, and the negative correlation with compatible elements, suggests joint magmatic evolution of these components and argues against late-stage hydrothermal leaching of boron from pelitic country rocks (Schneider and Lehmann 1977).

It is interesting to note that Li shows a negative correlation with B and other incompatible components. The Li pattern implies fractionation involving a Li-bearing mineral phase, such as mica, during quartz crystallization.

The linear log-log variation trends are typical of high-silica magma chambers with strong chemical gradients (Hildreth 1981). The fluid-dynamic mechanism behind this pattern is probably convective fractionation, i.e. convective separation of residual liquid from crystals (Sparks et al. 1984). Note that this kind of fractional crystallization is not related to crystal settling, sometimes misrepresented in the literature as synonymous with fractional crystallization. The alternative process of liquid-liquid fractionation by thermogravitational diffusion (Hildreth 1981) is less likely because the highly charged components, titanium and zirconium, show negative log-correlation trends with tantalum and other incompatible elements in the Bolivian tin porphyries (Dietrich et al. 1997).

The high abundances of fluid-mobile elements such as B, As and Li in least-fractionated melt samples allow an assessment of the source material. The Precambrian granulitic basement which is exposed near the Bolivia-

Chile border (Troeng et al. 1994) and in deep drillholes on the Altiplano (Lehmann 1978) is not a likely candidate for melt generation with high fluid-mobile elements because these components would have been easily mobilized during prograde metamorphism. This is why granulites are among the most B-deficient rocks known, with generally < 5 ppm B (Leeman and Sisson 1996).

The high levels of B and other volatile components in the melt inclusions of the Bolivian tin porphyries suggest an origin from first-cycle metamorphic rocks not yet depleted in this fluid-mobile element suite. A likely candidate for such a source material is the Lower Paleozoic meta-sedimentary sequence which commonly forms the immediate host rocks to the currently exposed porphyry systems, but also to the 25–28 Ma granitic intrusives of the Cordillera Quimsa Cruz which may be a deeper equivalent of the younger tin porphyry systems further south (Fig. 1). The Lower Paleozoic meta-sedimentary sequence has a stratigraphic thickness of about 10,000 m and is folded and thrusted. Cenozoic E-W tectonic shortening of the Eastern Cordillera of central and southern Bolivia is estimated at roughly 30%, with a major detachment surface at 10–15 km depth on top of the Proterozoic basement (Kley et al. 1997). The present-day surface heat-flow in the Eastern Cordillera is roughly 80 mW/m² (Springer and Förster 1999) which would allow melting conditions near the Paleozoic/Proterozoic boundary and is consistent with a ponded basaltic melt in the middle or lower crust. Hot mafic magma in the root zones of silicic magma chambers is probably a general feature of Cordilleran magmatic systems where regions of thick continental crust may impede major basaltic penetration to shallow levels (Hildreth 1981).

The involvement of primitive magma in the tin porphyry systems is implied by their hybrid intermediate bulk compositions (Dietrich et al. 1997, 1999) and in their Nd isotope composition. Neodymium isotope data for some Bolivian tin porphyries are compiled in Table 2. Our reconnaissance Nd data from Llallagua, Chorolque and Cerro Rico de Potosí define an ε_{Nd} range of -5 to -10. The high-end data cover the -5 to -6 range for the 21-Ma Karikari igneous complex, near the Cerro Rico porphyry, and the Pliocene Los Frailes ignimbrite (Schneider 1985), whereas the low-end data are close to the values for the Macusani volcanic rocks

Table 2 Neodymium isotope data on the Bolivian tin belt

Sample	Locality	Sm (ppm)	Nd (ppm)	$^{147}\text{Sm}/^{144}\text{Nd}^{\text{a}}$	$^{143}\text{Nd}/^{144}\text{Nd}^{\text{b}}$	ε_{Nd} (T = 10 Ma)
L18b	Llallagua	10.805	10.521	0.6208	0.512117	-10.7
L18a	Llallagua	10.212	63.408	0.0974	0.512163	-9.1
L22	Llallagua	9.221	59.366	0.0939	0.512158	-9.2
C56	Chorolque	9.636	67.909	0.0857	0.512278	-6.9
C64	Chorolque	7.780	42.325	0.1111	0.512343	-5.7
P94a	Cerro Rico	9.787	74.683	0.0792	0.512357	-5.3
P95	Cerro Rico	5.781	39.046	0.0895	0.512140	-9.6

^a Analytical error is < 0.3% (2 σ)

^b Analytical error is < 0.006% (2 σ)

with $\varepsilon_{\text{Nd}} - 9$ (Pichavant et al. 1988). The Lower Paleozoic sequence of southern Peru and northern Bolivia has an ε_{Nd} range of -8 to -12 (Miller and Harris 1989; Basu et al. 1990). The Proterozoic basement rocks of the Altiplano, seen in gneiss cobbles in the Tertiary Azurita conglomerate and in three petroleum exploration drill-holes at core depths of 2400–2800 m, have ε_{Nd} values from -11 to -14 (T_{DM} around 1.9 Ga) (Aitcheson and Moorbat 1992, unpublished data). These data allow no clear-cut distinction between the Proterozoic basement and the Lower Paleozoic cover rocks but suggest that the Bolivian tin porphyry systems are dominantly of intracrustal origin. Nevertheless, the slightly less negative ε_{Nd} data for the tin porphyries compared to the Lower Paleozoic sequence indicate a variable mantle component of up to about 30% when calculated with the end-member ε_{Nd} values of $+8$ (MORB) and -10 (Bolivian upper crust).

The high abundances of B, Li, Cs, Rb and As in the melt inclusions from Bolivian tin porphyries characterize a highly evolved rhyolitic melt. The highly-fractionated nature of the melt inclusions was previously noted by Dietrich et al. (1997) and shown to contrast strongly with the dacitic bulk-rock composition of the Bolivian tin porphyries. Dietrich et al. (1999) assume mixing of rhyolitic melt and an inferred more mafic melt portion to explain the dacitic bulk-rock composition. The mixing event may be related to venting of a zoned magma chamber, or to intrusion of basaltic melt into a chemically independent silicic system.

Conclusions

Trace-element microanalysis of melt inclusions provides new insights into the magmatic evolution of strongly-altered porphyry systems. The Bolivian tin porphyries have chemical affinities with their thick pelitic host-rock sequence. High boron, lithium, cesium and arsenic contents characterize both quartz-hosted melt inclusions in Miocene porphyries and their Lower Paleozoic wall rocks. Incompatible (boron, arsenic, cesium, rubidium) and compatible (titanium, zirconium) components in melt inclusions define systematic correlation trends over about one log unit which may be attributed to fractional crystallization. Lithium behaves as a compatible element, which is suggestive of fractionation of a Li-rich crystal phase, such as mica, during quartz crystallization.

Neodymium isotope data support a dominantly upper crustal source for the Bolivian tin porphyries. However, slightly less negative ε_{Nd} values in the porphyry systems as compared to the Bolivian upper crust suggest the involvement of up to 30% mantle component. The basaltic mantle-derived component is thought to have mixed with upper crustal rhyolitic melts and to have produced the hybrid dacitic bulk-rock composition of the tin porphyries (Dietrich et al. 1999). The mantle connection through thick back-arc continental crust provides the thermal basis for upper crustal melting,

with a long melt storage/residence time necessary for extended magmatic fractionation.

The pelitic source material provides not only the diagnostic fluid-mobile B-Li-Cs-As element suite and the peraluminous nature of the melt systems, but the small carbon content of the dark sediments is also likely to imprint the reduced paleo-sedimentary environment onto the magmatic systems. This can explain the ilmenite-series affinity of the silicic rocks of the Bolivian tin belt, as opposed to the general magnetite-series affinity of copper porphyry systems (Lehmann 1994). The metallogenetic specialization of tin depends critically on the oxidation state of a melt system (Linnen et al. 1995), and incompatible behaviour of tin in silicic magma requires reducing conditions as manifested in ilmenite-series rocks. The Bolivian tin belt had suitable source lithologies and the appropriate heat supply from long-lived mantle-driven thermal anomalies to sustain upper-crustal silicic magma chambers with extended high-level crystal fractionation.

Acknowledgements This study is part of a long-term research effort on the metallogenesis of the central Andes, currently funded by Deutsche Forschungsgemeinschaft (Le-578/9-1) and Volkswagen-Stiftung (I-71649). We thank GEOBOL/SERGEOMIN under the Directors Franz Tavera and Marcelo Claure for logistical support during fieldwork, and Kurt Traxel (Heidelberg), Karsten Gömann and Klaus Hermann (Clausthal) for help with the proton and electron microprobes, respectively. Neodymium isotope analysis was done at the isotope geochemistry lab of the University of Göttingen in cooperation with Prof Bent Hansen. Reviews of the manuscript by Richard Sillitoe and Chris Halls are acknowledged with thanks.

References

- Ahlfeld F, Schneider-Scherbina A (1964) Los yacimientos minerales y de hidrocarburos de Bolivia. Bol Dep Nac Geol (La Paz) 5: 1–388
- Amlot R (1998) Tin. Mining J Lond (Suppl): 18–19
- Atkinson WW Jr, Souviron A, Vehrs TI, Faunes A (1996) Geology and mineral zoning of the Los Pelambres porphyry copper deposit, Chile. In: Camus F, Sillitoe R, Petersen R (eds) Andean copper deposits: new discoveries, mineralization, styles and metallogenesis. Soc Econ Geol Spec Publ 5: 131–155
- Basu AR, Sharma M, DeCelles PG (1990) Nd-, Sr-isotopic provenance and trace element geochemistry of Amazonian foreland basin fluvial sands, Bolivia and Peru: implications for ensialic Andean orogeny. Earth Planet Sci Lett 100: 1–17
- Clark AH, Farrar E, Caelles JC, Haynes SJ, Lortie RB, McBride SL, Quirt GS, Robertson RCR, Zentilli M (1976) Longitudinal variations in the metallogenetic evolution of the central Andes: a progress report. Geol Assoc Can Spec Pap 14: 23–58
- Clark AH, Palma VV, Archibald DA, Farrar E, Arenas FMJ, Robertson RCR (1983) Occurrence and age of tin mineralization in the Cordillera Oriental, southern Peru. Econ Geol 78: 514–520
- Clark AH, Archibald DA, Lee AW, Farrar E, Hodgson CJ (1998) Laser probe $^{40}\text{Ar}/^{39}\text{Ar}$ ages of early and late-stage alteration assemblages, Rosario porphyry copper-molybdenum deposit, Collaguasi district, I. Region, Chile. Econ Geol 93: 326–337
- Cunningham CG, Zartman RE, McKee EH, Rye RO, Naeser CW, Sanjines OV, Erickson GE, Tavera FV (1996) The age and thermal history of Cerro Rico de Potosí, Bolivia. Miner Deposita 31: 374–385

- Dietrich A (1999) Metallogenie, Geochemie und Schmelzeinschluss-Untersuchungen von tin porphyry und copper porphyry Lagerstätten der zentralen Anden (Bolivien, Chile). Clausthaler Geowiss Diss 57: 1–198
- Dietrich A, Lehmann B, Wallianos A, Traxel K (1997) The Lower Miocene tin porphyry system of Llallagua, Bolivia: bulk rock and melt inclusion geochemistry. In: Papunen H (ed) Mineral deposits: research and exploration – where do they meet? Proc 4th Biennial SGA Meeting, Turku, Finland, 11–13 Aug 1997, Balkema, Rotterdam, pp 625–628
- Dietrich A, Lehmann B, Wallianos A, Traxel K (1999) Magma mixing in Bolivian tin porphyries. *Naturwissenschaften* 86: 40–43
- Erickson GE, Luedke RG, Smith RL, Koeppen RP, Urquidi BF (1990) Peraluminous igneous rocks of the Bolivian tin belt. *Geology* 13: 3–8
- Everden JF, Kriz SJ, Cherroni C (1977) Potassium-argon ages of some Bolivian rocks. *Econ Geol* 72: 1042–1061
- Francis PW, Halls C, Baker MCW (1983) Relationships between mineralization and silicic volcanism in the central Andes. *J Volcanol Geotherm Res* 18: 165–190
- Grant JN, Halls C, Avila W, Avila G (1977) Igneous geology and the evolution of hydrothermal systems in some sub-volcanic tin deposits of Bolivia. *Geol Soc Lond Spec Publ* 7: 117–126
- Grant JN, Halls C, Avila W, Snelling NJ (1979) K-Ar ages of igneous rocks and mineralization in part of the Bolivian tin belt. *Econ Geol* 74: 838–851
- Grant JN, Halls C, Sheppard SMF, Avila W (1980) Evolution of the porphyry tin deposits of Bolivia. *Mining Geol Spec Issue* 8: 151–173
- Halls C (1994) Energy and mechanism in the magmatic-hydrothermal evolution of the Cornubian batholith: a review. In: Seltmann R, Kämpf H, Möller P (eds) Metallogenesis of collisional orogens. Czech Geol Surv, Prague, pp 274–294
- Hildreth W (1981) Gradients in silicic magma chambers: implications for lithospheric magmatism. *J Geophys Res* 86 (B11): 10153–10192
- Kelly WC, Turneaure FS (1970) Mineralogy, paragenesis and geothermometry of the tin and tungsten deposits of the eastern Andes, Bolivia. *Econ Geol* 65: 609–680
- Kley J, Müller S, Tawackoli S, Jacobshagen V, Manutsoglu E (1997) Pre-Andean and Andean-age deformation in the Eastern Cordillera of Bolivia. *J S Am Earth Sci* 10: 1–19
- Leeman WP, Sisson VB (1996) Geochemistry of boron and its implications for crustal and mantle processes. *Rev Mineral* 33: 645–707
- Lehmann B (1978) A Precambrian core sample from the Altiplano, Bolivia. *Geol Rundsch* 67: 270–278
- Lehmann B (1982) Metallogenesis of tin: magmatic differentiation versus geochemical heritage. *Econ Geol* 77: 50–59
- Lehmann B (1985) Formation of the strata-bound Kellhuani tin deposits, Bolivia. *Miner Deposita* 20: 169–176
- Lehmann B (1994) Petrochemical factors governing the metallogenesis of the Bolivian tin belt. In: Reutter KJ, Scheuber E, Wigger PJ (eds) Tectonics of the central Andes. Springer, Berlin Heidelberg New York, pp 317–326
- Lehmann B, Ishihara S, Michel H, Miller J, Sanchez A, Tistl M, Winkelmann L (1990) The Bolivian tin province and regional tin distribution in the central Andes: a reassessment. *Econ Geol* 85: 1044–1058
- Lehmann B, Petersen U, Santivanez R, Winkelmann L (1988) Distribución geoquímica de estano y boro en la secuencia paleozoíca inferior de la Cordillera Real de Bolivia. *Bol Soc Geol Perú* 77: 19–27
- Linnen RL, Pichavant M, Holtz F, Burgess S (1995) The effect of f_{O_2} on the solubility, diffusion, and speciation of tin in haplogranitic melt at 850 °C and 2 kbar. *Geochim Cosmochim Acta* 59: 1579–1588
- Manning DAC, Pichavant M (1988) Volatiles and their bearing on the behavior of metals in granitic systems. In: Taylor RP, Strong DF (eds) Recent advances in the geology of granite-related mineral deposits. *CIM Spec Vol* 39: 13–24
- McBride SL, Robertson RCR, Clark AH, Farrar E (1983) Magmatic and metallogenetic episodes in the northern tin belt, Cordillera Real, Bolivia. *Geol Rundsch* 72: 685–713
- Métrich N, Joron JL, Berthier B (1998) Occurrence of boron-rich potassic melts in the Vulsini volcanic district, Italy: evidence from melt inclusions. *Geochim Cosmochim Acta* 62: 507–514
- Miller JF, Harris NBW (1989) Evolution of continental crust in the central Andes; constraints from Nd isotope systematics. *Geology* 17: 615–617
- Morgan VI GB, London D, Luedke RG (1998) Petrochemistry of late Miocene peraluminous silicic volcanic rocks from the Morococala Field, Bolivia. *J Petrol* 39: 601–632
- Morris J, Leeman WP, Tera F (1990) The subducted component in island arc lavas: constraints from Be isotopes and B-Be systematics. *Nature* 344: 31–36
- Mosbah M, Clochetti R, Métrich N, Piccot D, Rio S, Tirira J (1995) The characterization of glass inclusions through nuclear microprobe. *Nucl Instruments Methods Phys Res B* 104: 271–275
- Noble DC, Vogel TA, Peterson PS, Landis GP, Grant NK, Jezek PA, McKee EH (1984) Rare-element enriched, S-type ash-flow tuffs containing phenocrysts of muscovite, andalusite, and sillimanite, southeastern Peru. *Geology* 12: 35–39
- Palacios C, Townley B, Héral G (1999) Geology and geochemistry of Upper Jurassic and Early Cretaceous mesothermal gold mineralization in the Coastal Range, central Chile. *J Geochem Explor* (in press)
- Pichavant M, Valencia HJ, Boulmier S, Briqueu L, Joron JL, Juteau M, Marin L, Michard A, Sheppard SMF, Treuil M, Vernet M (1987) The Macusani glasses, SE Peru: evidence of chemical fractionation in peraluminous magmas. In: Mysen BO (ed) Magmatic processes: physicochemical principles. *Geochem Soc Spec Publ* 1: 359–373
- Pichavant M, Kontak DJ, Briqueu L, Valencia Herrera J, Clark AH (1988) The Miocene-Pliocene Macusani volcanics, SE Peru. II. Geochemistry and origin of a felsic peraluminous magma. *Contrib Mineral Petrol* 100: 325–338
- Pollard PJ, Pichavant M, Charoy B (1987) Contrasting evolution of fluorine- and boron-rich tin systems. *Miner Deposita* 22: 315–321
- Rio S, Métrich N, Mosbah M, Massiot P (1995) Lithium, boron and beryllium in volcanic glasses and minerals studied by nuclear microprobe. *Nucl Instruments Methods Phys Res B* 100: 141–148
- Ryan JG, Morris J, Tera F, Leeman WP, Tsvetkov A (1995) The slab effect as a function of depth: evidence from cross-arc geochemical variation in the Kurile Arc. *Science* 270: 625–627
- Ryan JG, Leeman WP, Morris J, Langmuir CH (1996) The boron systematics of intraplate lavas: implications for crust and mantle evolution. *Geochim Cosmochim Acta* 60: 415–422
- Schneider A (1985) Eruptive processes, mineralization and isotopic evolution of the Los Frailes-Karikari region/Bolivia. PhD Thesis, Univ London, 280 pp
- Schneider HJ, Lehmann B (1977) Contribution to a new genetic concept on the Bolivian tin province. In: Klemm DD, Schneider HJ (eds) Time- and strata-bound ore deposits. Springer, Berlin Heidelberg New York, pp 153–168
- Serrano L, Vargas R, Stambuk V, Aguilar C, Galeb M, Holmgren C, Contreras A, Godoy S, Vela I, Skewes MA, Stern CR (1996) The late Miocene to Early Pliocene Rio Blancos-Los Bronces copper deposit, central Chilean Andes. In: Camus F, Sillitoe R, Petersen R (eds) Andean copper deposits: new discoveries, mineralization, styles and metallogenesis. *Soc Econ Geol Spec Publ* 5: 119–129
- Sillitoe RH (1976) Andean mineralization: a model for the metallogenesis of convergent plate margins. *Geol Assoc Can Spec Pap* 14: 59–100
- Sillitoe RH (1988) Epochs of intrusion-related copper mineralization in the Andes. *J S Am Earth Sci* 1: 89–108
- Sillitoe RH, Sawkins FJ (1971) Geologic, mineralogic and fluid inclusion studies relating to the origin of copper-bearing tourmaline breccia pipes, Chile. *Econ Geol* 66: 1028–1041

- Sillitoe RH, Halls C, Grant JN (1975) Porphyry tin deposits in Bolivia. *Econ Geol* 70: 913–927
- Sillitoe RH, Steele GB, Thompson JFH, Lang JR (1998) Advanced argillic lithocaps in the Bolivian tin-silver belt. *Miner Deposita* 33: 539–546
- Skewes MA, Stern CR (1995) Genesis of the giant late Miocene to Pliocene copper deposits of central Chile in the context of Andean magmatic and tectonic evolution. *Int Geol Rev* 37: 893–909
- Smith HJ, Spivack AJ, Staudigel H, Hart SR (1995) The boron isotopic composition of altered oceanic crust. *Chem Geol* 126: 119–135
- Sparks RSJ, Huppert HE, Turner JS (1984) The fluid dynamics of evolving magma chambers. *Philos Trans R Soc Lond A* 310: 511–534
- Springer M, Förster A (1999) Heat-flow density across the central Andean subduction zone. *Tectonophysics* (in press)
- Taylor RG (1979) Geology of tin deposits. Elsevier, Amsterdam, 543 pp
- Taylor SR, McLennan SM (1985) The continental crust: its composition and evolution. Blackwell, Oxford, 312 pp
- Traxel K, Arndt P, Bohsung J, Braun-Dullaeus KU, Maetz M, Reimold D, Schiebler H, Wallianos A (1995) The Heidelberg proton microprobe: the success of a minimal concept. *Nucl Instruments Methods Phys Res B* 104: 19–25
- Troeng B, Soria EE, Claure VH, Mobarac R, Murillo F (1994) Descubrimiento de basamento precámbrico en la Cordillera Occidental, Altiplano de los Andes bolivianos. Mem XI Congr Geol Bolív, Santa Cruz, 6–9 Oct 1994, pp 231–237
- Wallianos A (1998) Mikroanalytik an magmatischen Schmelzeinschlüssen und spezielle Probleme bei der Datenauswertung von PIXE-Spektren. PhD Thesis, Univ Heidelberg, 125 pp
- Webster JD, Burt DM, Aguillon RA (1996) Volatile and lithophile trace-element geochemistry of Mexican tin rhyolite magmas deduced from melt inclusions. *Geochim Cosmochim Acta* 60: 3267–3283
- Webster JD, Thomas R, Rhede D, Förster HJ, Seltmann R (1997) Melt inclusions in quartz from an evolved peraluminous pegmatite: geochemical evidence for strong tin enrichment in fluorine-rich and phosphorus-rich residual melts. *Geochim Cosmochim Acta* 61: 2589–2604
- Winkelmann L (1983) Geologie und Lagerstätten im Bereich Palca (Mururata) und die Geochemie der Silursedimentite in der Cordillera La Paz/Bolivien. Berl Geowiss Abh A 51: 1–110